

# HetEmotionNet: Two-Stream Heterogeneous Graph Recurrent Neural Network for Multi-modal Emotion Recognition

Ziyu Jia

ziyujia@bjtu.edu.cn

School of Computer and Information Technology, Beijing Jiaotong University & Beijing Key Laboratory of Traffic Data Analysis and Mining Beijing, China

Youfang Lin

yflin@bjtu.edu.cn

School of Computer and Information Technology, Beijing Jiaotong University & Beijing Key Laboratory of Traffic Data Analysis and Mining & CAAC Key Laboratory of Intelligent Passenger Service of Civil Aviation Beijing, China

Jing Wang\*

wj@bjtu.edu.cn

School of Computer and Information Technology, Beijing Jiaotong University & Beijing Key Laboratory of Traffic Data Analysis and Mining & CAAC Key Laboratory of Intelligent Passenger Service of Civil Aviation Beijing, China

Zhiyang Feng

zhiyangfeng@bjtu.edu.cn

School of Computer and Information Technology, Beijing Jiaotong University Beijing, China

Xiangheng Xie

xiangheng@bjtu.edu.cn

School of Computer and Information Technology, Beijing Jiaotong University Beijing, China

Caijie Chen

caijiechen@bjtu.edu.cn

School of Computer and Information Technology, Beijing Jiaotong University Beijing, China

## ABSTRACT

The research on human emotion under multimedia stimulation based on physiological signals is an emerging field, and important progress has been achieved for emotion recognition based on multi-modal signals. However, it is challenging to make full use of the complementarity among spatial-spectral-temporal domain features for emotion recognition, as well as model the heterogeneity and correlation among multi-modal signals. In this paper, we propose a novel two-stream heterogeneous graph recurrent neural network, named HetEmotionNet, fusing multi-modal physiological signals for emotion recognition. Specifically, HetEmotionNet consists of the spatial-temporal stream and the spatial-spectral stream, which can fuse spatial-spectral-temporal domain features in a unified framework. Each stream is composed of the graph transformer network for modeling the heterogeneity, the graph convolutional network for modeling the correlation, and the gated recurrent unit for capturing the temporal domain or spectral domain dependency. Extensive experiments on two real-world datasets demonstrate that our proposed model achieves better performance than state-of-the-art baselines.

\*corresponding author

Permission to make digital or hard copies of all or part of this work for personal or classroom use is granted without fee provided that copies are not made or distributed for profit or commercial advantage and that copies bear this notice and the full citation on the first page. Copyrights for components of this work owned by others than ACM must be honored. Abstracting with credit is permitted. To copy otherwise, or republish, to post on servers or to redistribute to lists, requires prior specific permission and/or a fee. Request permissions from [permissions@acm.org](https://permissions.acm.org).  
MM '21, October 20–24, 2021, Virtual Event, China

© 2021 Association for Computing Machinery.  
ACM ISBN 978-1-4503-8651-7/21/10...\$15.00  
<https://doi.org/10.1145/3474085.3475583>

## CCS CONCEPTS

• **Computing methodologies** → *Neural networks*; • **Information systems** → *Multimedia information systems*; • **Human-centered computing** → *HCI design and evaluation methods*.

## KEYWORDS

Multi-modal emotion recognition; Graph recurrent neural network; Affective computing; Heterogeneous graph

## ACM Reference Format:

Ziyu Jia, Youfang Lin, Jing Wang, Zhiyang Feng, Xiangheng Xie, and Caijie Chen. 2021. HetEmotionNet: Two-Stream Heterogeneous Graph Recurrent Neural Network for Multi-modal Emotion Recognition. In *Proceedings of the 29th ACM International Conference on Multimedia (MM '21)*, October 20–24, 2021, Virtual Event, China. ACM, New York, NY, USA, 11 pages. <https://doi.org/10.1145/3474085.3475583>

## 1 INTRODUCTION

Emotion is a mental and physiological state which results from many senses and thoughts [10]. In recent years, emotion plays an increasingly important role in multiple areas, such as disease detection, human-computer interaction (HCI), and virtual reality. To collect data for emotion recognition, researchers often utilize multiple multimedia materials to stimulate participants and induce emotion. For the reason that videos, audio, and so on have the advantage of easy collection, there is a mass of studies using these data. Though they achieve certain performance, these data cannot guarantee to reflect a real emotional state since human can disguise their facial expression, sound, and so on. Physiological signals cannot be disguised, so they can reflect human emotion objectively. Therefore, physiological signals are more suitable for emotion recognition.

To achieve better performance for emotion recognition, some methods are proposed which use physiological signals and achieve

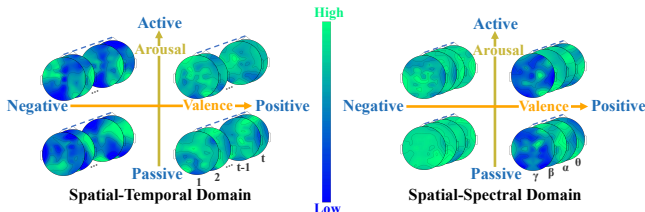


**Figure 1: The complementarity among spatial-spectral-temporal domain features.** The brain topographic maps indicate that there are differences of activation degree between temporal domain information and spectral domain information on the spatial domain for different emotional states which are categorized by valence and arousal. These differences in spatial-spectral-temporal domain information are complementary for emotion recognition.

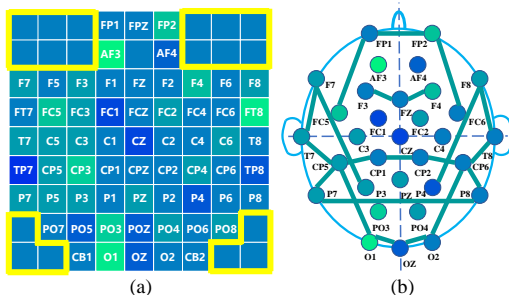


**Figure 2: Two different EEG representations.** (a) The 2D map of EEG signals. The EEG signals are constructed into image-like data and CNN is applied to extract features from these data. However, those marginal areas circled by the yellow border are often filled with zero, which may introduce noise and limit the performance of CNN. Because the voltage of these areas not covered by biosensors is usually not zero, artificial zero-filling may introduce wrong information. (b) The graph of EEG signals. The graph method preserves the functional connectivity among the electrodes to the greatest extent and does not introduce noise.

state-of-the-art performance [12, 34, 45]. However, several challenges still exist for emotion recognition using physiological signals.

**C1: How to utilize the complementarity among spatial-spectral-temporal domain information efficiently.** Temporal domain information and spectral domain information in the spatial domain of physiological signals usually have different activation degree. For example, Figure 1 indicates the differences between the temporal domain and the spectral domain in the spatial domain of electroencephalography (EEG) signals for different emotional states. To be specific, in the spatial-temporal domain, the activation degree of the temporal domain information directly reflects brain activity. The high degree of activation is usually related to positive emotion and the low degree of activation is often related to negative emotion. In the spatial-spectral domain, the activation degree of the  $\gamma$  band is often high in negative emotions and low in positive emotions [35]. Considering these phenomena, most studies design various deep learning methods to extract spatial-temporal domain information or spatial-spectral domain information for emotion recognition. These

methods can be mainly divided into two categories. One concentrates on the spatial-temporal domain [6, 25, 40, 47], and the other one concentrates on the spatial-spectral domain [49, 51, 56, 57]. Specifically, the methods focusing on spatial-temporal domain information often only take the raw signals or other statistical features as the input of the network. The methods focusing on the spatial-spectral domain often capture the correlation of the spectral domain features such as power spectral density (PSD) and differential entropy (DE) in the physiological signals. Though these two categories of methods achieve relatively satisfactory performance, they ignore complementarity among spatial-spectral-temporal domain information. SST-EmotionNet is proposed to extract the spatial-spectral-temporal domain information in the image-like maps [12]. However, areas of brain that are not covered by biosensors also produce bioelectrical signals. The voltage of these signals is usually not 0, so artificial zero-filling may introduce noise, as shown in Figure 2(a). Besides, in Figure 2(b), the graph-based method can reflect the topological relationship of the brain [17, 48]. These shortcomings limit the performance of classification to a certain extent. Therefore, how to effectively extract spatial-spectral-temporal domain information is challenging work.



**Figure 3: The heterogeneity of the multi-modal physiological signals.** For instance, there are differences in the waveform and amplitude between ECG and EEG signals.

**C2: How to model heterogeneity and correlation among different modalities simultaneously.** The heterogeneity and the correlation exist in multi-modal physiological signals. The heterogeneity among modalities is reflected in the differences among the attributes of various signals, which are collected from different organs [19]. For instance, electrocardiography (ECG) and EEG signals have a great difference in waveform and amplitude, as shown in Figure 3. The correlation includes intra-modality correlation and cross-modality correlation. The intra-modality correlation is the relationship among channels in the same modality, such as the functional connectivity as shown in Figure 2(b). The cross-modality correlation is the relationship among channels in different modalities. For example, when participants are in fear, a greater heart rate acceleration is reflected in ECG signals, accompanied by an increase in GSR signals, and high activation degree of EEG signals in the right frontal lobe [23, 26]. However, most current methods only model the heterogeneity or correlation among different modalities separately. As for the heterogeneity, existing works use different feature extractors, such as CNN, to extract features of different modalities and capture the heterogeneity in multi-modal data [27, 29, 34, 36]. However, these methods ignore the correlation among different modalities because the signals of different modalities are extracted separately. As for the correlation, existing works usually combine the signals of different modalities into a new data representation and feed it to a deep neural network to capture the correlation [30, 38], such as group sparse canonical correlation analysis (GSCCA) [55]. However, these methods ignore the heterogeneity among different modalities because the

features of all modalities are extracted by the same feature extractor. Therefore, how to model the heterogeneity and correlation among multi-modal signals simultaneously becomes a challenge.

To address these challenges, we propose a two-stream heterogeneous graph recurrent neural network named HetEmotionNet, which is composed of the spatial-temporal stream and spatial-spectral stream and takes heterogeneous graph sequences as input. A stream consists of a graph transformer network (GTN), a graph convolutional network (GCN), and a gated recurrent unit (GRU). The physiological signals are constructed into heterogeneous graph sequences as the input of our model. Several heterogeneous graphs are stacked to form a heterogeneous graph sequence. A heterogeneous graph consists of nodes and edges. A node represents a channel of signals whose type depends on the modality of the channel. An edge represents the connection between two nodes. To sum up, the main contributions of our work are summarized as follows:

- We propose a novel graph-based two-stream structure composed of the spatial-temporal stream and the spatial-spectral stream which can simultaneously fuse spatial-spectral-temporal domain features of physiological signals in a unified deep neural network framework.
- Each stream consists of a GTN for modeling the heterogeneity, a GCN for modeling the correlation, and a GRU for capturing the temporal or spectral dependency.
- Extensive experiments are conducted on two benchmark datasets to evaluate the performance of the proposed model. The results indicate the proposed model outperforms all the state-of-the-art models.

## 2 RELATED WORK

In recent years, time series analysis has attracted the attention of many researchers [13, 14]. As a typical time series, physiological signals are used in many fields, such as sleep staging [4, 11, 15, 17, 18], motor imagery [16, 24, 61], seizure detection [31, 32], and emotion recognition [12, 41, 57], etc. The physiological signals have been applied in emotion recognition widely because they can accurately reflect real emotions. Musha et al. use EEG signals to recognize emotions for the first time [37]. In the early stage of research, researchers adopted traditional machine learning models like SVM to extract features of EEG signals to recognize emotions [28]. However, those methods are often limited by prior knowledge. Deep learning methods [33, 41, 44, 45, 57, 59] are proposed to make up for the shortcomings of traditional machine learning methods. They have shown outstanding results in natural language processing [1] and computer vision [42] as well as in affective computing.

**Multi-domain Features Extraction.** In building deep learning models for emotion recognition, researchers often extract spatial-temporal domain features or spatial-spectral domain features to train models. For instance, for **spatial-temporal domain features** extraction, Zhang et al. propose a spatial-temporal recurrent neural network combining the spatial RNN layer and the temporal RNN layer to capture the spatial and temporal features, respectively [54]. Yang et al. propose a parallel convolutional recurrent neural network, which utilizes CNN to extract spatial features from data frames and RNN to extract temporal features from EEG signals [50]. For **spatial-spectral domain features** extraction, Yang

et al. propose a 3D EEG representation, which combines features from different frequency bands while retaining spatial information among channels [49]. Zheng et al. utilize Short-Time Fourier Transform with a non-overlapped Hanning window to extract features from multi-channel EEG signals and calculate DE features for each frequency band to predict the positive and negative emotional states [60]. Further, Jia et al. present SST-EmotionNet, extracting spatial features, spectral features, and temporal features simultaneously, and achieving higher performance for emotion recognition. However, image-like maps introduce noise into the network [12].

**Multi-modal Physiological Signals.** Most methods model either heterogeneity [29, 36] or correlation [38] to fuse multi-modal signals. For instance, for the **heterogeneity of multi-modal data**, Lin et al. extract the features of EEG signals and Peripheral Physiological Signals (PPS) separately, and then concatenate these features to model the heterogeneity of multi-modal signals for emotion recognition [27]. Ma et al. design a multi-modal residual LSTM network (MMResLSTM) for emotion recognition. The signals of different modalities are fed into different LSTM branches to extract multi-modal features [34]. For the **correlation of multi-modal data**, Zhang et al. adopt GSCCA to learn the correlation by extracting the group structure information between EEG signals and eye movement features [55]. Liu et al. fuse features of EEG signals and features of other modalities with bimodal deep autoencoders and then obtain the share representation [30].

Overall, existing emotion recognition methods have achieved high accuracy. However, they still ignore the fusion of multi-domain features, multi-modal heterogeneity, and correlation. To solve the limitations, we propose HetEmotionNet, which models the complementarity among spatial-spectral-temporal domain features, the heterogeneity, and the correlation of the signals simultaneously.

## 3 PRELIMINARIES

**Definition 1. Heterogeneous Graph.** We define  $G = (V, E)$  as a graph, where  $V$  denotes the node set and  $E$  denotes the edge set. The network schema is defined as  $\mathcal{T}_G = (\mathcal{A}, \mathcal{R})$ , where  $\mathcal{A}$  is the node type set and  $\mathcal{R}$  is the edge type set. We define  $\phi : V \rightarrow \mathcal{A}$  as the node type mapping and  $\psi : E \rightarrow \mathcal{R}$  as the edge type mapping. Therefore, a network can be defined as  $G = (V, E, \phi, \psi)$ . For a heterogeneous network  $G = (V, E, \phi, \psi)$ ,  $|\mathcal{A}| + |\mathcal{R}| > 2$ .

**Definition 2. Heterogeneous Emotional Network.** The heterogeneous emotional network  $G^{ER} = (V', E', \phi', \psi')$  is constructed based on multi-modal signals. We define  $V' = (v_1, v_2, \dots, v_N)$  as the node set, where the node  $v_i$  denotes a channel of physiological signals. The edge represents a connection relationship between two different channels.  $E' = (e_1, e_2, \dots, e_n)$  is defined as the edge set, where  $n$  is the number of edges. The number of node types is equal to the number of modalities. When the number of modalities is  $A'$ , the number of edge types is  $R' = A'(A' + 1)/2$ . After the node type mapping  $\phi' : V' \rightarrow A'$  and the edge type mapping  $\psi' : E' \rightarrow R'$  are defined, we construct the heterogeneous emotional network  $G^{ER} = (V', E', \phi', \psi')$ . In addition, the heterogeneous emotional network can be defined as  $G^{ER} = (X^F, A)$ , where  $X^F$  denotes the features of each node and  $A$  denotes the adjacency matrix of  $G^{ER}$ .

**Definition 3. Heterogeneous Graph Sequence.** We define  $G_s = (G_1, G_2, \dots, G_n)$  as a heterogeneous graph sequence, where  $n$

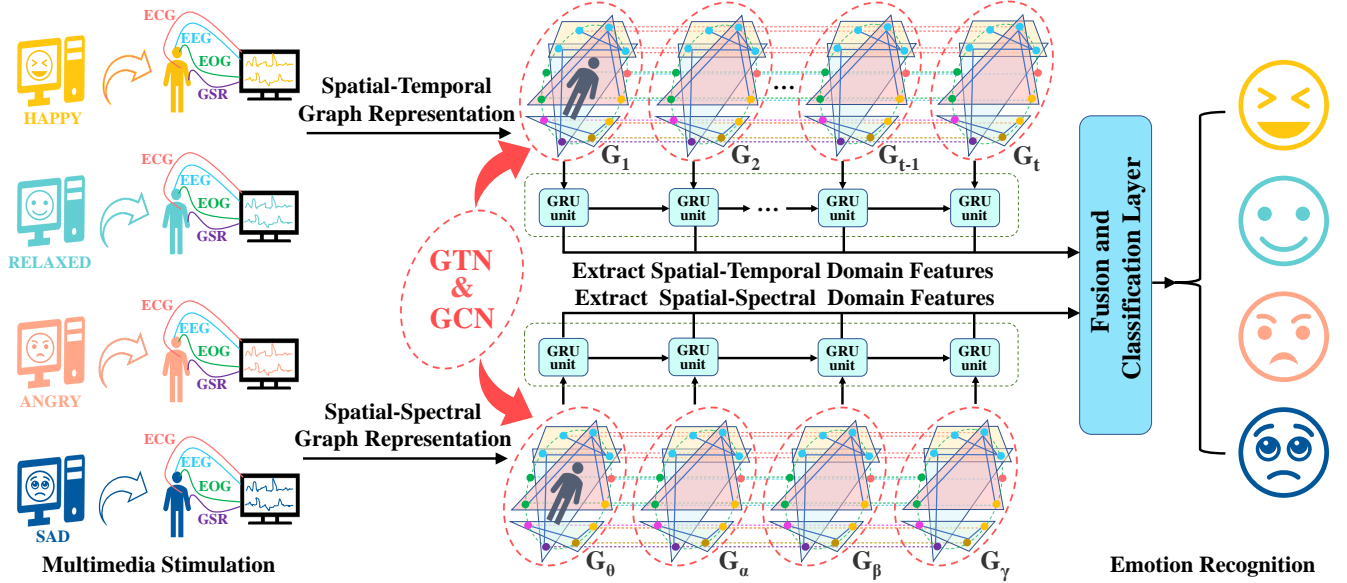


Figure 4: The whole schematic process for multi-modal emotion recognition. We obtain the multi-modal signals from the subjects and construct the graph sequence representation for the HetEmotionNet. HetEmotionNet consists of spatial-temporal stream and spatial-spectral stream. The two streams have the same structure. Each stream is composed of graph transformer network (GTN), graph convolutional network (GCN), and gated recurrent unit (GRU).

is the number of heterogeneous graphs. For instance, we construct the spatial-temporal graph sequence  $G^T = (G_1, G_2, \dots, G_T) \in \mathbb{R}^{N \times T}$ , where  $T$  denotes the number of the timesteps in the sample. Analogously, we construct the spatial-spectral graph sequence  $G^B = (G_1, G_2, \dots, G_B) \in \mathbb{R}^{N \times B}$ , where  $B$  is the number of frequency bands.

**Problem Statement.** Our research goal is to learn a mapping function between graph sequences and emotional states. Given spatial-temporal graph sequence  $G^T$  and spatial-spectral graph sequence  $G^B$ , the emotion recognition problem can be defined as  $Y = F(G^T, G^B)$ , where  $Y$  denotes the emotion classification and  $F$  denotes the mapping function.

## 4 METHODOLOGY

Figure 4 illustrates the overall structure of our model. We propose a HetEmotionNet based on the constructed graph sequence from the multi-modal signals. HetEmotionNet consists of a spatial-temporal stream and a spatial-spectral stream, and these two streams have the similar structure. Each stream of HetEmotionNet is composed of graph transformer network, graph convolutional network, and gated recurrent unit. We summarize five core ideas of HetEmotionNet: 1) Design a heterogeneous graph-based spatial-spectral-temporal representation for multi-modal emotion recognition. 2) Integrate the graph-based spatial-temporal stream and spatial-spectral stream in a unified network structure to extract spatial-spectral-temporal domain features simultaneously. 3) Adopt graph transformer network to model the heterogeneity of multi-modal signals. 4) Apply graph convolutional network to capture the correlation among different channels. 5) Employ the gated recurrent unit to capture temporal domain or spectral domain dependency, respectively.

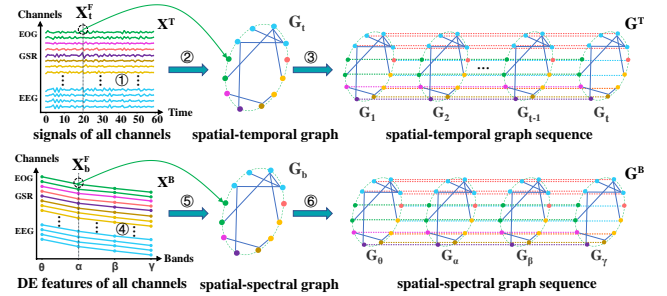


Figure 5: The schematic process of heterogeneous graph sequence construction. The heterogeneous graph sequence is stacked by several heterogeneous graphs. A heterogeneous graph is composed of the node features and graph structure. Each node corresponds to a channel, whose node type depends on the modality of channel. Graph structure represents the relationship among channels.

### 4.1 Heterogeneous Graph Sequence Construction

For each sample, we construct a heterogeneous spatial-temporal graph sequence and a heterogeneous spatial-spectral graph sequence separately as shown in Figure 5. These heterogeneous graph sequences are used to describe the spatial distribution of the temporal domain and spectral domain information of multi-modal signals. The heterogeneous graph sequence is made up of several heterogeneous graphs. The general heterogeneous graph is usually defined as  $G = (X^F, A)$ , where  $X^F$  denotes the graph node features,  $A$  denotes the graph adjacency matrix which describes the relationship of channels. Besides, the node type depends on the modality of the channel.

Figure 5 presents the process of constructing the heterogeneous graph sequence. Firstly, we build the relationship of the channels as ① in Figure 5. Specifically, we calculate the correlation degree among different channels in the sample to determine the relationship of the channels using mutual information [22]. Formally, given a channel pair  $(u, v)$ , their correlation  $a_{u,v}$  can be formulated as follows:

$$a_{u,v} = I(X_u^T; X_v^T) = \sum_{m \in X_u^T} \sum_{n \in X_v^T} p(m, n) \log \frac{p(m, n)}{p(m)p(n)}, \quad (1)$$

where  $1 \leq u \leq N$ ,  $1 \leq v \leq N$ ,  $X_u^T$  represents the signals of channel  $u$ ,  $X_v^T$  represents the signals of channel  $v$ ,  $T$  is the number of timesteps, and  $N$  is the number of channels. After calculating the correlation degree for all the channel pairs, we obtain the adjacency matrix  $A = (a_{1,1}, \dots, a_{u,v}, \dots, a_{N,N}) \in \mathbb{R}^{N \times N}$  of the spatial-temporal graphs and the spatial-spectral graphs.

To construct the heterogeneous spatial-temporal graph sequence, we compute the temporal node features  $X_t^F = (X_t^{F1}, X_t^{F2}, \dots, X_t^{FN}) \in \mathbb{R}^N$ , where  $X_t^{Fi}$  denotes the amplitude ( $\mu V$ ) on the  $i^{th}$  channel in the  $t^{th}$  timestep from the multi-modal signals,  $1 \leq t \leq T$ . Then, we combine the temporal domain feature vector  $X_t^F$  and the adjacency matrix  $A$  to form a heterogeneous spatial-temporal graph  $G_t = (X_t^F, A)$  as ②. Therefore, we obtain  $T$  heterogeneous spatial-temporal graphs from the sample. These heterogeneous spatial-temporal graphs are stacked into a heterogeneous spatial-temporal graph sequence  $G^T = (G_1, G_2, \dots, G_{T-1}, G_T)$  as ③.

To construct the heterogeneous spatial-spectral graph sequence, similar to the process of generating heterogeneous spatial-temporal graph sequence, we extract the DE features from the  $B \in \mathbb{Z}^+$  frequency bands in the sample as ④. These features extracted from different channels and the correlation among channels are converted to heterogeneous spatial-spectral graphs. Specifically, these feature vectors extracted from  $N$  channels in the  $b^{th}$  frequency band  $X_b^F = (X_b^{F1}, X_b^{F2}, \dots, X_b^{FN}) \in \mathbb{R}^N$  and the adjacency matrix  $A$  of the sample are composed of a heterogeneous spatial-spectral graph  $G_b = (X_b^F, A)$  as ⑤. Therefore, we obtain  $B$  heterogeneous spatial-spectral graphs in  $B$  frequency bands for each sample. Then, these heterogeneous spatial-spectral graphs are stacked into a heterogeneous spatial-spectral sequence  $G^B = (G_\theta, G_\alpha, G_\beta, G_\gamma)$  as ⑥.

## 4.2 Heterogeneous Graph Recurrent Neural Network

HetEmotionNet consists of graph transformer network and graph recurrent neural network. Graph recurrent neural network is composed of graph convolutional network and gated recurrent unit.

**Graph Transformer Network.** The Graph Transformer Network (GTN) [52] is used to model the heterogeneity of multi-modal signals by automatically extracting the meta-paths from the adjacency matrix set  $\mathcal{A}$ . Specifically,  $\mathcal{A}$  is generated from the heterogeneous adjacency matrix obtained in Section 4.1. The heterogeneous adjacency matrix is divided into homogeneous adjacency matrix set  $\mathcal{A} = \{\mathcal{A}_1, \mathcal{A}_2, \dots, \mathcal{A}_{N_a}\}$  according to edge types, where  $\mathcal{A}_i$  is homogeneous adjacency matrix,  $1 \leq i \leq N_a$ , and  $N_a$  is the number of adjacency matrices which is decided by the number of edge types.

GTN consists of several GT-layers. Each GT-layer aims to learn a two-level meta-path, which represents the second-order neighbor relationship in the graph by learning two graph structures from  $\mathcal{A}$ . GT-layer has two steps: the first step is designed to softly construct two graph structures, which are defined as:

$$Q_1 = \phi(\mathcal{A}, \text{softmax}(W_{\phi_1})), \quad (2)$$

$$Q_2 = \phi(\mathcal{A}, \text{softmax}(W_{\phi_2})), \quad (3)$$

where  $\phi$  denotes the  $1 \times 1$  convolution,  $W_{\phi_1} \in \mathbb{R}^{1 \times 1 \times K}$  and  $W_{\phi_2} \in \mathbb{R}^{1 \times 1 \times K}$  are the parameters of  $\phi$ .  $Q_1$  and  $Q_2$  are the graph structures constructed by the  $1 \times 1$  convolution.

The second step is designed to generate meta-paths by matrix multiplication of  $Q_1$  and  $Q_2$ . Formally,  $H^{(l)} = Q_1 Q_2$ , where  $H^{(l)}$  represents the meta-paths generated by  $l^{th}$  GT-layer. For calculation stability,  $H^{(l)}$  is updated as  $H^{(l)} = D^{-1} Q_1 Q_2$ , where  $D$  denotes the degree matrices of  $\mathcal{A}$ .

Stacking several GT-layers in GTN aims to learn a high-level meta-path that is a useful relationship of multi-modal signals. The  $l^{th}$  GT-layer in GTN updates the graph structure and multiplies the graph structure with the one constructed by  $(l-1)^{th}$  GT-layer. Formally,  $H^{(l)} = Q_l H^{(l-1)}$ , where  $Q_l$  denotes the graph structure learned by  $l^{th}$  GT-layer,  $H^{(l)}$  and  $H^{(l-1)}$  represent the meta-paths learned by  $(l-1)^{th}$  and  $l^{th}$  GT-layers, respectively. To consider multiple relationship of multi-modal signals, which are decided by the number of meta-paths simultaneously, multi-channel  $1 \times 1$  convolution is applied. The graph structure generated by multi-channel  $1 \times 1$  convolution is defined as:

$$Q'_l = \Phi(\mathcal{A}, \text{softmax}(W_\Phi)), \quad (4)$$

where  $\Phi$  is the multi-channel  $1 \times 1$  convolution,  $W_\Phi \in \mathbb{R}^{1 \times C^A \times K}$  is learnable parameter,  $C^A$  is the number of channels, and  $Q'_l$  is the graph structure generated from  $l^{th}$  GT-layer by this convolution. To concurrently learn various lengths of meta-paths, the identity matrix is added into the result of each GT-layer. Finally, the graph sequence is updated into  $C^A$  sequences according to the meta-paths learned from GTN.

**Graph Recurrent Neural Network.** Graph recurrent neural network has two chief components, namely graph convolutional network and gated recurrent unit. These two components are used to extract both spatial domain and temporal/spectral domain features from graph sequences. Specifically, GCN is used to capture the spatial domain features by aggregating information from neighbor nodes. In addition, GRU is applied to extract temporal/spectral domain features from the graph sequence obtained after GCN.

*Graph Convolutional Network.* GCN captures the correlation among the nodes in the graph. The correlation is valuable to recognize different emotions. For example, there exists much functional connectivity among different brain regions. Capturing the spatial domain relationship among these functional connectivity contributes to recognizing different emotions.

To capture the correlation, the spectral graph theory extends the convolution operation from image-like data to graph structure data [3]. The graph structure is represented by its Laplacian matrix in the spectral graph analysis. The Laplacian matrix and its eigenvalues reflect the property of the graph. The Laplacian matrix is defined as  $L = D - A$ , where  $L \in \mathbb{R}^{N \times N}$  is the Laplacian matrix,  $A \in \mathbb{R}^{N \times N}$  is

the adjacency matrix,  $D \in \mathbb{R}^{N \times N}$  is the degree matrix of the graph, and  $N$  is the vertex number. The eigenvalues matrix is obtained by decomposing the Laplacian matrix with  $L = U\Lambda U^T$ , where  $U$  is the Fourier basis and  $\Lambda \in \mathbb{R}^{N \times N}$  is a diagonal matrix. The node feature is defined as  $x_i \in \mathbb{R}^N$  for the graph  $G_i$  in graph sequence  $G_s$ . Then, the graph Fourier transform and inverse Fourier transform are defined as  $\hat{x}_i = U^T x_i$  and  $x_i = U\hat{x}_i$ , respectively. Because the graph convolution operation is equal to the product of these signals which have been transformed into the spectral domain [3], the graph convolution of signals  $x_i$  on graph  $G_i$  is defined as:

$$g_\theta \star_{G_i} x_i = U g_\theta U^T x_i, \quad (5)$$

where  $g_\theta$  denotes a graph convolution kernel and  $\star_{G_i}$  denotes a graph convolution operation on graph  $G_i$ . In addition, to simplify the calculation of Laplace matrix, the  $K$  order Chebyshev Polynomials are adopted, which is defined as:

$$g_\theta(\Lambda) \approx \sum_{k=0}^K \theta_k T_k(\tilde{\Lambda}), \quad (6)$$

where  $\tilde{\Lambda} = \frac{2}{\lambda_{max}} \Lambda - I_N$ ,  $I_N$  is the identity matrix, and  $\lambda_{max}$  is the maximum eigenvalues of  $\Lambda$ . The  $\theta \in \mathbb{R}^K$  is a vector of polynomial coefficients. The Chebyshev polynomials are defined as  $T_k(x) = 2xT_{k-1}(x) - T_{k-2}(x)$  recursively, where  $T_0(x) = 1$  and  $T_1(x) = x$ . With the  $K$  order Chebyshev Polynomials, the message from 0 to  $K^{th}$  neighbours are aggregated into the center node. For the fast calculation [20], the first-order polynomials are used and  $\lambda_{max} = 2$ ,  $k = 1$  are set. Then, the graph convolution is further simplified as:

$$g_\theta \star_{G_i} x_i \approx \theta \left( I_N + D^{-\frac{1}{2}} A D^{-\frac{1}{2}} \right) x_i, \quad (7)$$

where  $D$  is the degree matrix,  $A$  is the adjacency matrix, and  $\theta$  is the parameter.  $I_N + D^{-\frac{1}{2}} A D^{-\frac{1}{2}}$  is changed into  $\tilde{D}^{-\frac{1}{2}} \tilde{A} \tilde{D}^{-\frac{1}{2}}$  to prevent numerical instability, gradient explosion and gradient disappearance, where  $\tilde{D} = \sum_j A_{ij}$  and  $\tilde{A} = A + I_N$ . The graph convolution of signals  $x_i$  on graph  $G_i$  in graph sequence is defined as:

$$H_i^{GCN} = \sigma \left( \tilde{D}^{-\frac{1}{2}} \tilde{A} \tilde{D}^{-\frac{1}{2}} x_i W \right) + b, \quad (8)$$

where  $x_i$  and  $H_i^{GCN}$  are the node features before and after the graph convolution, respectively.  $W$  is the weight vector,  $\sigma$  is the Rectified Linear Unit (ReLU) activation function, and  $b$  is a bias.

The graph convolution operation is applied to the graph sequence. Formally, for graph sequence  $G_s = \{G_1, G_2, \dots, G_{ns}\} \in \mathbb{R}^{N \times ns}$  and each graph  $G_i$  in  $G_s$ , the graph convolution operation is applied on  $G_i$ . After the graph convolution operation is performed on all graphs in  $G_s$ , the results are stacked together to construct a new graph sequence  $H_s = \{H_1, H_2, \dots, H_{ns}\} \in \mathbb{R}^{N \times ns}$ . To decrease the number of parameters, all graph convolution operations share the same parameters.

Since the meta-paths learned by GTN update the graph sequence obtained in Section 4.2 into  $C^A$  graph sequences, the graph convolution operation is performed on each of the graph sequences. Then, the weighted sum operation is adopted to concatenate the graph sequences together. The weighted sum operation on graph

sequences  $G_s^{GTN}$  is defined as:

$$H_s^{GCN} = \sum_i^{C^A} w_i \delta_s(G_{s_i}^{GTN}), \quad (9)$$

where  $\delta_s$  denotes the graph convolution operation on the graph sequence,  $w_i$  is the weight for the weighted sum operation, and  $G_{s_i}^{GTN}$  is the  $i^{th}$  graph sequence in  $G_s^{GTN}$ .

*Gated Recurrent Unit.* After the graph convolutional network, GRU is applied to capture the dependency among different timesteps or frequency bands. Gated recurrent unit consists of the reset gate and the update gate [5], which is defined as:

$$R_i = \sigma \left( W_r H_i^{GCN} + V_r H_{i-1}^{GRU} \right) + b_r, \quad (10)$$

$$\tilde{H}_i^{GCN} = \tanh \left( W_h H_i^{GCN} + V_h \left( R_i \odot H_{i-1}^{GRU} \right) + b_h \right), \quad (11)$$

$$Z_i = \sigma \left( W_z H_i^{GCN} + V_z H_{i-1}^{GRU} \right) + b_z, \quad (12)$$

$$H_i^{GRU} = (1 - Z_i) \odot \tilde{H}_i^{GCN} + Z_i \odot H_{i-1}^{GRU}, \quad (13)$$

where the parameters and the operator are defined as follows,

$\odot$ : the product of two matrices on each element.

$H_i^{GCN}$ : the  $i^{th}$  graph of the graph sequence, which is the input of the  $i^{th}$  GRU unit.

$H_{i-1}^{GRU}$ : the output of previous GRU unit, which is the input of the  $i^{th}$  GRU unit. It contains the information of the previous graphs.

$R_i$ : the output of the reset gate from  $H_i^{GCN}$  and  $H_{i-1}^{GRU}$ .

$\tilde{H}_i^{GCN}$ : the output of tanh activation controlled by the reset gate  $R_i$ , which determines the forgotten degree of the previous state  $H_{i-1}^{GRU}$ .

$Z_i$ : the output of the update gate, which determines how many elements of  $H_{i-1}^{GRU}$  and its state are updated in the  $i^{th}$  GRU unit.

$H_i^{GRU}$ : the output of the  $i^{th}$  GRU unit.

$W_r, V_r, W_h, V_h, W_z,$  and  $V_z$  are the learnable parameters of the GRU unit.

Each graph  $H_{st}^{GCN}$  in  $H_s^{GCN}$  is fed into the  $t^{th}$  GRU unit to capture the features among the graphs.  $H_s^{GRU}$  is obtained by concatenating all outputs of the GRU units together.

### 4.3 Fusion and Classification

The heterogeneous graph recurrent neural network is used to extract the spatial-temporal domain and spatial-spectral domain features of multi-modal data in the two streams, respectively. After extraction, the features obtained from the spatial-temporal and the spatial-spectral streams are fused, which are defined as:

$$H_3 = (H_1^{GRU} W_1 + b_1) \parallel (H_2^{GRU} W_2 + b_2), \quad (14)$$

$$Y = \text{softmax}(\text{ReLU}(H_3 W_3 + b_3) W_4 + b_4), \quad (15)$$

where  $\parallel$  denotes the concatenate operation,  $H_1^{GRU}$  and  $H_2^{GRU}$  denote the the features extracted by spatial-temporal and spatial-spectral stream, and  $Y$  denotes the classification result of our model.  $W_1, b_1, W_2, b_2, W_3, b_3, W_4,$  and  $b_4$  denote the learnable parameters of the classification layer. In this paper, the cross entropy [7] is applied as loss function.

## 5 EXPERIMENTS

### 5.1 Datasets

We conduct experiments on two datasets that contain the multi-modal physiological signals: DEAP [21] and the MAHNOB-HCI [43] datasets, which evoke emotion by multimedia materials.

**DEAP dataset** records the data generated by 32 participants under multimedia stimulation. Each participant needs to undergo 40 trials and watches a 1-minute music video during each trial. Their physiological signals are recorded while they are watching music videos, and data of each trial includes 3s pre-trial signals and 60s trial signals. The dataset contains 32-channel EEG signals and 8-channel Peripheral Physiological Signals (PPS). The peripheral physiological signals include EOG, EMG, GSR, BVP, respiration, and temperature. The music videos are rated on valence, arousal, and other emotional dimensions from 1 to 9 by all participants.

**MAHNOB-HCI dataset** records the data generated by 27 participants under multimedia stimulation. Each participant watches 20 video clips, while physiological data of 20 trials is recorded. The length of these video clips is between 34.9s and 117s (mean is 81.4s, standard deviation is 22.5s). The dataset contains 32-channel EEG signals and 6-channel PPS. The peripheral physiological signals include ECG, GSR, respiration, and temperature. Participants are required to score each video clip from 1 to 9 on the emotional dimensions of valence, arousal, etc.

### 5.2 Baseline Models and Settings

The baseline models include MLP [39], SVM [2], GCN [20], DGCNN [44], MM-ResLSTM [34], ACRNN [45], and SST-EmotionNet [12]. In order to make a fair comparison with the baseline methods, we perform the same data processing and experimental settings for all methods. Specifically, for the DEAP dataset, trials are applied the baseline reduction according to [50]. Then, a 1s non-overlapping window [46] is employed to divide each trial into several samples. For each sample, the Fourier transform with Hanning is utilized to extract the DE features [8, 58]. We compute DE features in four frequency bands for each channel. Due to the different attributes of different modal signals, we have adopted different frequency band division strategies for different modal signals. The specific division strategy is detailed in Table S.2 in the Supplementary Material. For the MAHNOB-HCI dataset, similar to the processing of the DEAP dataset, we employ the baseline reduction to each trial and extract the DE features in four frequency bands.

Our model is implemented with Pytorch framework and trained on NVIDIA 2080 Ti. The code has been released in GitHub<sup>1</sup>. The threshold is set as 5 to divide valence and arousal into two categories, respectively [21, 45]. Valence measures the pleasantness of emotion and arousal measures the intensity of emotion. We evaluate all methods using 10-fold cross-validation [9].

### 5.3 Results Analysis and Comparison

We compare our model with other baseline models on the DEAP dataset and the MAHNOB-HCI dataset, respectively.

Table 1 presents the average accuracy and standard deviation of these models for emotion recognition on the DEAP dataset. The

**Table 1: The performance on the DEAP dataset.**

Model	Valence (%)	Arousal (%)
MLP [39]	74.31±4.56	76.23±5.12
SVM [2]	83.14±3.66	84.50±4.43
GCN [20]	89.17±2.90	90.33±3.59
DGCNN [44]	90.44±3.01	91.70±3.46
MM-ResLSTM [34]	92.30±1.55	92.87±2.11
ACRNN [45]	93.72±3.21	93.38±3.73
SST-EmotionNet [12]	95.54±2.54	95.97±2.86
HetEmotionNet	<b>97.66±1.54</b>	<b>97.30±1.65</b>

**Table 2: The performance on the MAHNOB-HCI dataset.**

Model	Valence (%)	Arousal (%)
MLP [39]	72.84±6.88	73.61±10.75
SVM [2]	77.31±6.77	77.16±9.14
GCN [20]	81.31±6.09	83.43±7.50
DGCNN [44]	86.21±9.35	86.07±10.53
MM-ResLSTM [34]	89.46±8.64	89.66±8.09
ACRNN [45]	88.10±5.49	89.90±5.96
SST-EmotionNet [12]	90.06±4.80	88.37±7.19
HetEmotionNet	<b>93.95±3.38</b>	<b>93.90±3.04</b>

results indicate our model achieves the best performance on the DEAP dataset. Due to the advantages of automatic feature extraction, most deep learning models have achieved better performance than traditional methods (MLP and SVM). GCN extracts the spatial domain features from signals based on a fixed graph, while DGCNN can adaptively learn the intrinsic relationship of different channels by optimizing the adjacency matrix. Consequently, the performance of DGCNN is more accurate than GCN by around 1%. MM-ResLSTM uses deep LSTM with residual network to capture the temporal information in the multi-modal signals (EEG and PPS). Hence, MM-ResLSTM can extract more abundant features and perform better than GCN and DGCNN. Compared with MM-ResLSTM, ACRNN can capture both temporal domain and spatial domain information and achieve a better accuracy of 93.72%, 93.38% for valence and arousal. Further, SST-EmotionNet can extract the spatial-spectral-temporal domain information from EEG signals by 3D CNN, with the accuracy of 95.54% and 95.97%. Although SST-EmotionNet achieves relatively excellent performance, it does not utilize complementarity of multi-modal signals efficiently. Our proposed graph-based model can explore spatial-spectral-temporal domain information from multi-modal signals efficiently. Moreover, our model takes the heterogeneous information of different modalities into consideration. Therefore, our model can adequately learn comprehensive information for emotion recognition, achieving the highest accuracy on the DEAP dataset. Meanwhile, our model achieves the lowest standard deviation, which indicates the stability of our model is also satisfied. Besides, Table 2 presents the performance of all models on the MAHNOB-HCI dataset. Our model achieves the accuracy of 93.95% and 93.90% for valence and arousal, respectively. The performance of other baseline methods is between 72.84% and 90.06%. The results indicate that our model performs best on the MAHNOB-HCI dataset.

<sup>1</sup><https://github.com/ziyujia/HetEmotionNet>



Figure 6: Ablation studies on different components.

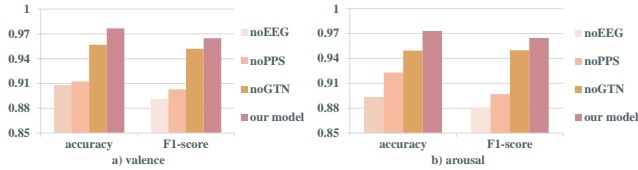


Figure 7: Ablation studies on fusing different modalities.

## 5.4 Ablation Studies

To verify the effectiveness of our model, ablation experiments are performed on the DEAP dataset. There are three kinds of ablation experiments: 1) Ablation experiments on the effectiveness of graph transformer network, graph convolutional network, and gated recurrent unit. 2) Ablation experiments on the effectiveness of fusing different modalities. 3) Ablation experiments on two-stream structure to verify whether utilizing spatial-spectral-temporal domain features simultaneously is useful.

**Ablation on different components.** To verify the effectiveness of different components in our model, we design three variants, which are described as follows:

- **HetEmotionNet-noGRU:** To verify the effects of GRU on capturing temporal or spectral dependency, this variant removes GRU from HetEmotionNet.
- **HetEmotionNet-noGTN:** To verify the effectiveness of GTN on modeling the heterogeneity of multi-modal data, this variant removes GTN from HetEmotionNet.
- **HetEmotionNet-noGCN:** To verify the effectiveness of GCN on capturing the correlation, we remove GCN from HetEmotionNet.

Figure 6 presents that removing different components from HetEmotionNet reduces the performance. HetEmotionNet outperforms HetEmotionNet-noGTN, which indicates that GTN is effective to model the heterogeneity of multi-modal data. HetEmotionNet has a better performance than HetEmotionNet-noGCN, demonstrating that GCN is effective to capture the correlation among channels. By comparing HetEmotionNet and HetEmotionNet-noGRU, it presents that HetEmotionNet-noGRU performs worse than HetEmotionNet, which indicates that GRU is important to capture the temporal or spectral dependency and improves the performance of model.

**Ablation on fusing data of different modalities.** To verify the effects of using multi-modal data and modeling the heterogeneity of multi-modal data, we conduct ablation experiments and design three variants of HetEmotionNet:

- **HetEmotionNet-noEEG:** It removes EEG signals from the multi-modal data to verify the effects of only using PPS on the model’s performance. In addition, we remove GTN from this variant because GTN is used to model the heterogeneity of multi-modal data while this variant only uses PPS.
- **HetEmotionNet-noPPS:** It removes PPS from the multi-modal data to verify the influences of only using EEG signals on the model’s performance. We remove the GTN for the same reason of HetEmotionNet-noEEG.

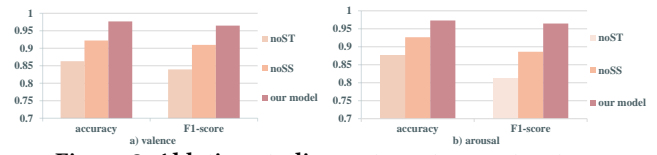


Figure 8: Ablation studies on two-stream structure.

- **HetEmotionNet-noGTN:** It uses both EEG signals and PPS. However, it removes GTN to verify that modeling the heterogeneity of multi-modal data is important.

As Figure 7 illustrates, HetEmotionNet-noPPS performs better than HetEmotionNet-noEEG. This result indicates that the effects of only using EEG signals is better than only using PPS, because EEG signals are the main physiological signals used in emotion recognition [53]. Besides, HetEmotionNet-noGTN outperforms HetEmotionNet-noPPS and HetEmotionNet-noEEG, which demonstrates that fusing data of different modalities further improves the performance. However, HetEmotionNet-noGTN does not model the heterogeneity of multi-modal data. Therefore, HetEmotionNet is designed to model the heterogeneity of multi-modal data and reaches the best results.

**Ablation on two-stream structure.** To verify the effectiveness of integrating two-stream, we design two variants as follows:

- **HetEmotionNet-noST (Spatial-Temporal stream):** This variant removes the spatial-temporal stream to verify the effects of utilizing the spatial-temporal domain features of physiological signals.
- **HetEmotionNet-noSS (Spatial-Spectral stream):** This variant removes the spatial-spectral stream to verify the effects of using the spatial-spectral domain features of physiological signals.

As Figure 8 illustrates, HetEmotionNet-noSS performs better than HetEmotionNet-noST, which demonstrates that extracting features in spatial and temporal domain is more effective than extracting features in spatial and spectral domain. Besides, HetEmotionNet has a better performance than two variants, which manifests that our model is able to fuse the spatial-spectral-temporal domain features simultaneously and improve the classification accuracy.

## 6 CONCLUSION

In this paper, we propose a novel two-stream heterogeneous graph recurrent neural network using multi-modal physiological signals for emotion recognition. The proposed HetEmotionNet is based on the two-stream structure, which can extract spatial-spectral-temporal domain features from multi-modal signals simultaneously. Moreover, each stream consists of GTN for modeling the heterogeneity, GCN for modeling the correlation, and GRU for capturing the temporal domain or spectral domain dependency. Experiments on the DEAP and the MAHNOB-HCI datasets indicate that our proposed model achieves state-of-the-art performance on DEAP and MAHNOB-HCI. Besides, the proposed model is a general framework for multi-modal physiological signals.

## ACKNOWLEDGMENTS

Financial supports by National Natural Science Foundation of China (61603029), the Fundamental Research Funds for the Central Universities (2020YJS025), and the China Scholarship Council (202007090056) are gratefully acknowledged. We are grateful for supporting from Swarna-Kaifeng Workshop which is sponsored by Swarna Club and Kaifeng Foundation.

## REFERENCES

- [1] Dzmitry Bahdanau, Kyunghyun Cho, and Yoshua Bengio. Neural machine translation by jointly learning to align and translate. *arXiv preprint arXiv:1409.0473*, 2014.
- [2] Bernhard E Boser, Isabelle M Guyon, and Vladimir N Vapnik. A training algorithm for optimal margin classifiers. In *Proceedings of the fifth annual workshop on Computational learning theory*, pages 144–152, 1992.
- [3] Joan Bruna, Wojciech Zaremba, Arthur Szlam, and Yann LeCun. Spectral networks and locally connected networks on graphs. *arXiv preprint arXiv:1312.6203*, 2013.
- [4] Xiyang Cai, Ziyu Jia, Minfang Tang, and Gaoxing Zheng. Brainsleepnet: Learning multivariate eeg representation for automatic sleep staging. In *2020 IEEE International Conference on Bioinformatics and Biomedicine (BIBM)*, pages 976–979. IEEE, 2020.
- [5] Junyoung Chung, Caglar Gulcehre, KyungHyun Cho, and Yoshua Bengio. Empirical evaluation of gated recurrent neural networks on sequence modeling. *arXiv preprint arXiv:1412.3555*, 2014.
- [6] Muhammad Najam Dar, Muhammad Usman Akram, Sajid Gul Khawaja, and Amit N Pujari. Cnn and lstm-based emotion charting using physiological signals. *Sensors*, 20(16):4551, 2020.
- [7] Pieter-Tjerk De Boer, Dirk P Kroese, Shie Mannor, and Reuven Y Rubinfeld. A tutorial on the cross-entropy method. *Annals of operations research*, 134(1):19–67, 2005.
- [8] Ruo-Nan Duan, Jia-Yi Zhu, and Bao-Liang Lu. Differential entropy feature for eeg-based emotion classification. In *2013 6th International IEEE/EMBS Conference on Neural Engineering (NER)*, pages 81–84. IEEE, 2013.
- [9] Gene H Golub, Michael Heath, and Grace Wahba. Generalized cross-validation as a method for choosing a good ridge parameter. *Technometrics*, 21(2):215–223, 1979.
- [10] William James. *What is an Emotion?* Simon and Schuster, 2013.
- [11] Ziyu Jia, Xiyang Cai, Gaoxing Zheng, Jing Wang, and Youfang Lin. Sleepprintnet: A multivariate multimodal neural network based on physiological time-series for automatic sleep staging. *IEEE Transactions on Artificial Intelligence*, 1(3):248–257, 2020.
- [12] Ziyu Jia, Youfang Lin, Xiyang Cai, Haobin Chen, Haijun Gou, and Jing Wang. Sst-emotionnet: Spatial-spectral-temporal based attention 3d dense network for eeg emotion recognition. In *Proceedings of the 28th ACM International Conference on Multimedia*, pages 2909–2917, 2020.
- [13] Ziyu Jia, Youfang Lin, Zehui Jiao, Yan Ma, and Jing Wang. Detecting causality in multivariate time series via non-uniform embedding. *Entropy*, 21(12):1233, 2019.
- [14] Ziyu Jia, Youfang Lin, Yunxiao Liu, Zehui Jiao, and Jing Wang. Refined nonuniform embedding for coupling detection in multivariate time series. *Physical Review E*, 101(6):062113, 2020.
- [15] Ziyu Jia, Youfang Lin, Jing Wang, Xuehui Wang, Peiyi Xie, and Yingbin Zhang. Salientsleepnet: Multimodal salient wave detection network for sleep staging. *arXiv preprint arXiv:2105.13864*, 2021.
- [16] Ziyu Jia, Youfang Lin, Jing Wang, Kaixin Yang, Tianhang Liu, and Xinwang Zhang. Mmccnn: A multi-branch multi-scale convolutional neural network for motor imagery classification. In Frank Hutter, Kristian Kersting, Jeffrey Lijffijt, and Isabel Valera, editors, *Machine Learning and Knowledge Discovery in Databases*, pages 736–751, Cham, 2021. Springer International Publishing.
- [17] Ziyu Jia, Youfang Lin, Jing Wang, Ronghao Zhou, Xiaojun Ning, Yuanlai He, and Yaoshuai Zhao. Graphsleepnet: Adaptive spatial-temporal graph convolutional networks for sleep stage classification. In *IJCAI*, pages 1324–1330, 2020.
- [18] Ziyu Jia, Youfang Lin, Hongjun Zhang, and Jing Wang. Sleep stage classification model based on deep convolutional neural network. *Journal of Zhejiang University (Engineering Science)*, 54(10):1899–1905, 2020.
- [19] Yingying Jiang, Wei Li, M Shamim Hossain, Min Chen, Abdulhameed Alelaiwi, and Muneer Al-Hammadi. A snapshot research and implementation of multimodal information fusion for data-driven emotion recognition. *Information Fusion*, 53:209–221, 2020.
- [20] Thomas N Kipf and Max Welling. Semi-supervised classification with graph convolutional networks. *arXiv preprint arXiv:1609.02907*, 2016.
- [21] Sander Koelstra, Christian Muhl, Mohammad Soleymani, Jong-Seok Lee, Ashkan Yazdani, Touradj Ebrahimi, Thierry Pun, Anton Nijholt, and Ioannis Patras. Deap: A database for emotion analysis; using physiological signals. *IEEE transactions on affective computing*, 3(1):18–31, 2011.
- [22] Alexander Kraskov, Harald Stögbauer, and Peter Grassberger. Estimating mutual information. *Physical review E*, 69(6):066138, 2004.
- [23] Sylvia D Kreibitz. Autonomic nervous system activity in emotion: A review. *Biological psychology*, 84(3):394–421, 2010.
- [24] Zhenqi Li, Jing Wang, Ziyu Jia, and Youfang Lin. Learning space-time-frequency representation with two-stream attention based 3d network for motor imagery classification. In *2020 IEEE International Conference on Data Mining (ICDM)*, pages 1124–1129. IEEE, 2020.
- [25] Jinxiang Liao, Qinghua Zhong, Yongsheng Zhu, and Dongli Cai. Multimodal physiological signal emotion recognition based on convolutional recurrent neural network. In *IOP Conference Series: Materials Science and Engineering*, volume 782, page 032005. IOP Publishing, 2020.
- [26] Antje Lichtenstein, Astrid Oehme, Stefan Kupschick, and Thomas Jürgensohn. Comparing two emotion models for deriving affective states from physiological data. In *Affect and emotion in human-computer interaction*, pages 35–50. Springer, 2008.
- [27] Wenqian Lin, Chao Li, and Shouqian Sun. Deep convolutional neural network for emotion recognition using eeg and peripheral physiological signal. In *International Conference on Image and Graphics*, pages 385–394. Springer, 2017.
- [28] Yi-Lin Lin and Gang Wei. Speech emotion recognition based on hmm and svm. In *2005 international conference on machine learning and cybernetics*, volume 8, pages 4898–4901. IEEE, 2005.
- [29] Wei Liu, Jie-Lin Qiu, Wei-Long Zheng, and Bao-Liang Lu. Multimodal emotion recognition using deep canonical correlation analysis. *arXiv preprint arXiv:1908.05349*, 2019.
- [30] Wei Liu, Wei-Long Zheng, and Bao-Liang Lu. Multimodal emotion recognition using multimodal deep learning. *arXiv preprint arXiv:1602.08225*, 2016.
- [31] Yunxiao Liu, Youfang Lin, Ziyu Jia, Yan Ma, and Jing Wang. Representation based on ordinal patterns for seizure detection in eeg signals. *Computers in Biology and Medicine*, 126:104033, 2020.
- [32] Yunxiao Liu, Youfang Lin, Ziyu Jia, Jing Wang, and Yan Ma. A new dissimilarity measure based on ordinal pattern for analyzing physiological signals. *Physica A: Statistical Mechanics and its Applications*, 574:125997, 2021.
- [33] Yifei Lu, Wei-Long Zheng, Binbin Li, and Bao-Liang Lu. Combining eye movements and eeg to enhance emotion recognition. In *IJCAI*, volume 15, pages 1170–1176. Citeseer, 2015.
- [34] Jiaxin Ma, Hao Tang, Wei-Long Zheng, and Bao-Liang Lu. Emotion recognition using multimodal residual lstm network. In *Proceedings of the 27th ACM International Conference on Multimedia*, pages 176–183, 2019.
- [35] Nicola Martini, Danilo Menicucci, Laura Sebastiani, Remo Bedini, Alessandro Pingitore, Nicola Vanello, Matteo Milanese, Luigi Landini, and Angelo Gemignani. The dynamics of eeg gamma responses to unpleasant visual stimuli: From local activity to functional connectivity. *NeuroImage*, 60(2):922–932, 2012.
- [36] Trisha Mittal, Uttaran Bhattacharya, Rohan Chandra, Aniket Bera, and Dinesh Manocha. M3er: Multiplicative multimodal emotion recognition using facial, textual, and speech cues. In *Proceedings of the AAAI Conference on Artificial Intelligence*, volume 34, pages 1359–1367, 2020.
- [37] Toshimitsu Musha, Yumiko Terasaki, Hasnine A Haque, and George A Ivamitsky. Feature extraction from eegs associated with emotions. *Artificial Life and Robotics*, 1(1):15–19, 1997.
- [38] Joana Pinto, Ana Fred, and Hugo Plácido da Silva. Biosignal-based multimodal emotion recognition in a valence-arousal affective framework applied to immersive video visualization. In *2019 41st Annual International Conference of the IEEE Engineering in Medicine and Biology Society (EMBC)*, pages 3577–3583. IEEE, 2019.
- [39] David E Rumelhart, Geoffrey E Hinton, and Ronald J Williams. Learning internal representations by error propagation. Technical report, California Univ San Diego La Jolla Inst for Cognitive Science, 1985.
- [40] Elham S Salama, Reda A El-Khoribi, Mahmoud E Shoman, and Mohamed A Wahby Shalaby. Eeg-based emotion recognition using 3d convolutional neural networks. *Int. J. Adv. Comput. Sci. Appl*, 9(8):329–337, 2018.
- [41] Annett Schirmer and Ralph Adolphs. Emotion perception from face, voice, and touch: comparisons and convergence. *Trends in cognitive sciences*, 21(3):216–228, 2017.
- [42] Karen Simonyan and Andrew Zisserman. Very deep convolutional networks for large-scale image recognition. *arXiv preprint arXiv:1409.1556*, 2014.
- [43] Mohammad Soleymani, Jeroen Lichtenauer, Thierry Pun, and Maja Pantic. A multimodal database for affect recognition and implicit tagging. *IEEE transactions on affective computing*, 3(1):42–55, 2011.
- [44] Tengfei Song, Wenming Zheng, Peng Song, and Zhen Cui. Eeg emotion recognition using dynamical graph convolutional neural networks. *IEEE Transactions on Affective Computing*, 2018.
- [45] Wei Tao, Chang Li, Rencheng Song, Juan Cheng, Yu Liu, Feng Wan, and Xun Chen. Eeg-based emotion recognition via channel-wise attention and self attention. *IEEE Transactions on Affective Computing*, 2020.
- [46] Xiao-Wei Wang, Dan Nie, and Bao-Liang Lu. Emotional state classification from eeg data using machine learning approach. *Neurocomputing*, 129:94–106, 2014.
- [47] Zhiyuan Wen, Ruifeng Xu, and Jiachen Du. A novel convolutional neural networks for emotion recognition based on eeg signal. In *2017 International Conference on Security, Pattern Analysis, and Cybernetics (SPAC)*, pages 672–677. IEEE, 2017.
- [48] Zonghan Wu, Shirui Pan, Fengwen Chen, Guodong Long, Chengqi Zhang, and S Yu Philip. A comprehensive survey on graph neural networks. *IEEE transactions on neural networks and learning systems*, 2020.
- [49] Yilong Yang, Qingfeng Wu, Yazhen Fu, and Xiaowei Chen. Continuous convolutional neural network with 3d input for eeg-based emotion recognition. In *International Conference on Neural Information Processing*, pages 433–443. Springer, 2018.

- [50] Yilong Yang, Qingfeng Wu, Ming Qiu, Yingdong Wang, and Xiaowei Chen. Emotion recognition from multi-channel eeg through parallel convolutional recurrent neural network. In *2018 International Joint Conference on Neural Networks (IJCNN)*, pages 1–7. IEEE, 2018.
- [51] Yu-Xuan Yang, Zhong-Ke Gao, Xin-Min Wang, Yan-Li Li, Jing-Wei Han, Norbert Marwan, and Jürgen Kurths. A recurrence quantification analysis-based channel-frequency convolutional neural network for emotion recognition from eeg. *Chaos: An Interdisciplinary Journal of Nonlinear Science*, 28(8):085724, 2018.
- [52] Seongjun Yun, Minbyul Jeong, Raehyun Kim, Jaewoo Kang, and Hyunwoo J Kim. Graph transformer networks. *arXiv preprint arXiv:1911.06455*, 2019.
- [53] Jianhua Zhang, Zhong Yin, Peng Chen, and Stefano Nichele. Emotion recognition using multi-modal data and machine learning techniques: A tutorial and review. *Information Fusion*, 59:103–126, 2020.
- [54] Tong Zhang, Wenming Zheng, Zhen Cui, Yuan Zong, and Yang Li. Spatial-temporal recurrent neural network for emotion recognition. *IEEE transactions on cybernetics*, 49(3):839–847, 2018.
- [55] Xiaowei Zhang, Jing Pan, Jian Shen, Zia Ud Din, Junlei Li, Dawei Lu, Manxi Wu, and Bin Hu. Fusing of electroencephalogram and eye movement with group sparse canonical correlation analysis for anxiety detection. *IEEE Transactions on Affective Computing*, 2020.
- [56] Yuxuan Zhao, Xinyan Cao, Jinlong Lin, Dunshan Yu, and Xixin Cao. Multi-modal emotion recognition model using physiological signals. *arXiv preprint arXiv:1911.12918*, 2019.
- [57] Wei-Long Zheng, Wei Liu, Yifei Lu, Bao-Liang Lu, and Andrzej Cichocki. Emotionmeter: A multimodal framework for recognizing human emotions. *IEEE transactions on cybernetics*, 49(3):1110–1122, 2018.
- [58] Wei-Long Zheng and Bao-Liang Lu. Investigating critical frequency bands and channels for eeg-based emotion recognition with deep neural networks. *IEEE Transactions on Autonomous Mental Development*, 7(3):162–175, 2015.
- [59] Wei-Long Zheng, Jia-Yi Zhu, and Bao-Liang Lu. Identifying stable patterns over time for emotion recognition from eeg. *IEEE Transactions on Affective Computing*, 10(3):417–429, 2017.
- [60] Wei-Long Zheng, Jia-Yi Zhu, Yong Peng, and Bao-Liang Lu. Eeg-based emotion classification using deep belief networks. In *2014 IEEE International Conference on Multimedia and Expo (ICME)*, pages 1–6. IEEE, 2014.
- [61] Jia Ziyu, Lin Youfang, Liu Tianhang, Yang Kaixin, Zhang Xinwang, and Wang Jing. Motor imagery classification based on multiscale feature extraction and squeeze-excitation model. *Journal of Computer Research and Development*, 57(12):2481, 2020.

# Supplementary Material

**Table S.1: Notations and explanations**

Notation	Explanation
$X^F$	Node features
$A$	Adjacency matrix
$G^{ER}$	Heterogeneous emotional network
$T$	Number of timesteps
$B$	Number of frequency bands
$G^T$	Spatial-temporal graph sequence
$G^B$	Spatial-spectral graph sequence
$X_u^T$	Signals of channel $u$
$a_{u,v}$	Correlation between channel pair $(u, v)$
$\mathcal{A}$	Homogeneous adjacency matrix set
$Q_l$	Graph structure generated in the $l^{th}$ GT-layer
$L$	Laplacian matrix
$D$	Degree matrix
$U$	Fourier basis
$g_\theta$	Graph convolution kernel
$K$	Order of Chebyshev Polynomials
$\sigma$	Activation function
$ns$	Number of graphs in a graph sequence
$C_A$	Number of channels
$R$	Output of the reset gate
$Z$	Output of the update gate
$W$	Weight vector
$b$	Bias vector
$\phi$	$1 \times 1$ convolution
$\Phi$	Multi-channel $1 \times 1$ convolution
$\odot$	Element-wise multiplication

**Table S.2: The division strategy of frequency bands for physiological signals in different modalities according to [14,34]. For different modalities, the Fourier transform with Hanning is utilized to extract the DE features in four different frequency bands.**

Modality	Frequency band 1	Frequency band 2	Frequency band 3	Frequency band 4
EEG	4-8	8-14	14-31	31-45
EOG	4-8	8-14	14-31	31-45
EMG	4-8	8-14	14-31	31-45
ECG	4-8	8-14	14-31	31-45
GSR	0-0.6	0.6-1.2	1.2-1.8	1.8-2.4
BVP	0-0.1	0.1-0.2	0.2-0.3	0.3-0.4
Respiration	0-0.6	0.6-1.2	1.2-1.8	1.8-2.4
Temperature	0-0.05	0.05-0.1	0.1-0.15	0.15-0.2